Electron Spin Resonance Studies on the Oxidation Mechanism of Sterically Hindered Cyclic Amines in TiO_2 Photocatalytic Systems

Yoshio Nosaka,* Hayato Natsui, Mariko Sasagawa, and Atsuko Y. Nosaka

Department of Chemistry, Nagaoka University of Technology, Kamitomioka, Nagaoka 940-2188, Japan

Received: March 21, 2006; In Final Form: May 6, 2006

A sterically hindered cyclic amine, 4-hydroxy-2,2,6,6-tetramethylpiperidine (HTMP), is converted to the corresponding aminoxyl radical (nitroxide radical), 4-hydroxy-2,2,6,6-tetramethyl piperidine 1-oxyl (TEMPOL radical) as a result of a photocatalytic reaction in TiO_2 aqueous suspension. The time profile of the radical formation and the effect of additives, such as SCN^-, I^-, methanol, and H_2O_2, on the initial formation rate were measured in order to elucidate the reaction mechanism. The experimental observations indicated that the direct photocatalytic oxidation of HTMP followed by reaction with O_2 is the dominant process in the formation of TEMPOL radicals. Electrochemical measurements showed that HTMP is oxidized at 0.7 V (vs NHE), which is consistent with the proposed mechanism. The possibility of other processes, involving reactions with singlet molecular oxygen, superoxide radical, and hydroxyl radical, were excluded from the reaction mechanism.

1. Introduction

Photoinitiated reactions with titanium dioxide (TiO_2) have been widely studied and have received much attention from the perspective of photocatalytic self-cleaning, because they can be used to decompose pollutants and mineralize wastewater.[1−3] One of the most useful functions of TiO_2 photocatalysts is to decompose malodorous substances and thus to neutralize their odor, which has been applied commercially to air purifiers.[3] Many malodorous substances are amines. The amino groups in amines are usually more resistive to photocatalytic decomposition than other functional groups. For example, in the photocatalytic decomposition of ethanolamine, oxidation takes place mainly at the $-CH_2OH$ group, and the amino group remains during the degradation of the aliphatic alcohol.[4]

Since cyclic secondary amines with sterically hindered groups are known to oxidatively convert to stable nitroxide radicals, they are used as stabilizers to inhibit the chemical and photochemical degradation of high-density polypropylenes.[5] The stabilization is based on the radical transfer to the cyclic amines to form stable nitroxide radicals. The nitroxide radicals are so stable that they are commonly used as spin labels, for example, to provide information on the local mobility of macromolecules[6] and have also been reported to be candidate materials for polymer radical batteries, on the basis of their reversible redox properties.[7]

Several reaction mechanisms have been reported in the formation of nitroxide radicals from sterically hindered cyclic amines. For the detection of OH radicals, the formation of nitroxide radicals can be used as a nonconventional spin-trapping tool for the electron spin resonance (ESR) method.[8] Detection of singlet molecular oxygen ($^1O_2$) produced with anthraquinone photosensitizers was also accomplished by use of the formation of nitroxide radicals from hindered cyclic amines.[9,10] Furthermore, it has been reported that the superoxide radical ($\cdot O_2^-$) reacts with dialkyl secondary amines to form nitroxide radicals.[11] Direct oxidation of sterically hindered cyclic amines with ionizing radiation followed by reaction with molecular oxygen also produces the corresponding nitroxide radicals.[12] Since the literature shows that reactions with $\cdot$OH, $^1O_2$, and $\cdot O_2^-$ and direct surface oxidation all can be key processes for radical formation from cyclic amines, the reaction pathway in the formation of nitroxide radicals may depend on the reaction conditions. Thus, it is important to specify the active agent to form nitroxide radicals in the individual reaction system.

SCHEME 1

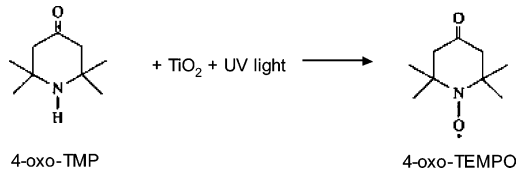

In TiO_2 photocatalytic systems, a few reports[13−15] have been published recently on the detection of the nitroxide radical, 4-oxo-2,2,6,6-tetramethylpiperidine-1-oxyl (4-oxo-TEMPO) from the sterically hindered cyclic amine 4-oxo-2,2,6,6-tetramethylpiperidine (4-oxo-TMP), as shown in Scheme 1. In a study in which the spin trapping reagent for $\cdot$OH radicals, 5,5-dimethyl-pyrroline-*N*-oxide (DMPO), was simultaneously present, the formation of the DMPO $\cdot$OH radical adduct was also observed, in addition to the 4-oxo-TEMPO radical.[13] That report suggested that both the 4-oxo-TEMPO radical and the DMPO $\cdot$OH radical adduct were produced by $^1O_2$ in TiO_2 photocatalysis. By use of two kinds of sterically hindered cyclic amines, 2,2,6,6-tetramethylpiperidine (TMP) and 4-oxo-TMP, the formation of $^1O_2$ was proposed on the basis of a comparison of the photoreaction of TiO_2 with that of solid lignin polymer.[14] Formation of $^1O_2$ was suggested from the detection of 4-oxo-TEMPO and $\cdot O_2^-$ with the DMPO spin trap in a photocatalytic system modified with a carotenoid.[15] Thus, all of the relevant literature suggests the contribution of $^1O_2$ to the formation of nitroxide radicals in TiO_2 photocatalytic systems.

We have been studying the various active oxygen species formed in TiO_2 photocatalysis. By use of chemiluminescence probe methods, the amount and behavior of $\cdot O_2^-$ was investigated.[16] For the formation of an $\cdot$OH radical, several detection

* To whom correspondence should be addressed. E-mail: nosaka@nagaokaut.ac.jp. Fax: +81-258-47-9315.

10.1021/jp061765h CCC: $33.50
Published on Web 06/09/2006

methods, for example, those involving a DMPO spin trap, a nitroxide spin probe, and a terephthalic acid fluorescence probe, have been compared.[16] On the basis of the evidence, we concluded that the direct reaction of probing agents with surface holes could not be ignored in TiO_2 photocatalysis.[17] Furthermore, we proved the existence of $^1O_2$ by directly monitoring the phosphorescence at 1270 nm in a TiO_2 aqueous suspension.[18] Thus, $\cdot O_2^-$, ·OH, valence band holes(or surface trapped holes, h^+), and $^1O_2$ are well-known active species in TiO_2 photocatalytic systems. As mentioned above, with these active species nitroxide radicals can be formed from sterically hindered cyclic amines. Consequently, the detailed reaction mechanism of hindered cyclic amines is necessary in order to understand which species can be detected with cyclic amines by ESR spectrometers in TiO_2 photocatalytic systems. In the present study, to clarify the mechanism of the reaction from amines to nitroxide radicals, we measured the formation rate of nitroxide radicals in TiO_2 photocatalytic reactions under various conditions.

2. Experimental Section

2.1. Materials. The TiO_2 powders used in the present experiment are commercially available photocatalysts, which were Degussa P-25 (Nippon Aerosil), Hombikat UV-100 (Sachtleben Chemie), ST-21 (Ishihara Techno), F4 (Showa Titanium), AMT-100, AMT-600, and MT-500B (TAYCA). All TiO_2 powders were generous gifts from the corresponding manufacturers. 4-Hydroxy-2,2,6,6-tetramethylpiperidine (HTMP), 4-hydroxy-2,2,6,6-tetramethylpiperidine-1-oxyl (TEMPOL), 4-oxo-TMP hydrochloride, 4-oxo-TEMPO, and 1,4-diazabicyclo[2.2.2]-octane (DABCO) were purchased from Tokyo Kasei Co. Ltd., and used without further purification. The chloride-free form of 4-oxo-TMP reagent was obtained from the 4-oxo-TMP hydrochloride by neutralization with Na_2CO_3 aqueous solution, followed by extraction with chloroform and distillation. An aqueous solution of the commercial TEMPOL was used as a standard to measure the radical concentration. The diamagnetic impurity in the purchased TEMPOL reagent was measured to be 5% by use of NMR spectroscopy, with which only impurities having no electron spin can be detected. The ESR spectrum of the reagent consisted of only TEMPOL radical, with no paramagnetic impurities.

2.2. Methods. ESR spectra were recorded on a JEOL JES−RE2X spectrometer. In typical ESR experiments, TiO_2 powder was dispersed in a 2.5 cm^3 aliquot of an aqueous solution of 0.5 M (M = mol dm^{-3}) HTMP with ultrasonic agitation for 10 min, and then the suspension was introduced into a thin flat ESR cell (interior dimensions, $0.2 \times 5 \times 40$ mm^3). When the additives were tested, the TiO_2 suspension was kept in the dark for 24 h before the measurement to attain adsorption equilibrium on the TiO_2 surface. The ESR measurements were carried out under photoirradiation with a 500 W mercury lamp (Ushio USH-500D) through a band-pass filter (HOYA, U-350) and a mesh filter to attenuate the light intensity. The irradiation intensity was typically about 20 mW over a square area of 5 mm × 10 mm. Since the line width and line shape of the ESR signal remained unchanged under the same experimental conditions, the peak height of the signal for the nitroxide radical was taken to be proportional to the concentration. The ESR measurements for each suspension sample were performed three times at least, and the averaged value was plotted in figures. Since some TiO_2 powders could not maintain the uniform suspension in solution, the ESR measurements were completed as quickly as possible. Because of the instability of the suspension, the ESR signal intensity scattered by about 30% at most. Therefore, the three photocatalysts, P25, UV-100, and AMT-600, which maintain rather stable suspension, were mainly employed.

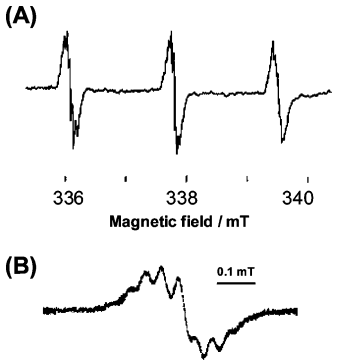

Figure 1. ESR spectrum observed with UV irradiation of a TiO_2 (4 g/L) aqueous suspension containing HTMP (0.1 M): microwave frequency, 9.45 GHz; modulation frequency, 100 kHz. Panel A shows modulation amplitude of 0.01 mT and microwave power at 1 mW. Panel B is an expanded scale view of one of the signals (low-field): field amplitude, 0.0025 mT; microwave power, 4 mW.

SCHEME 2

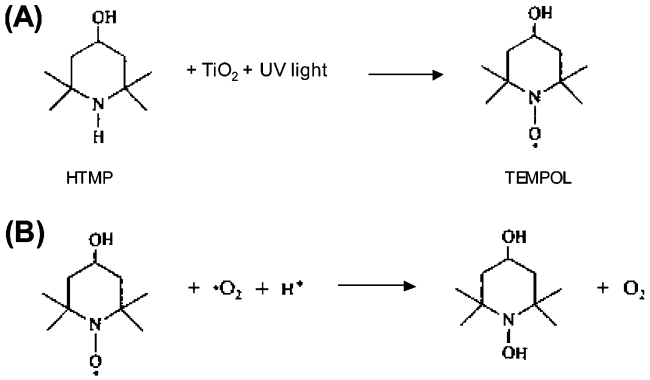

For electrochemical measurements, the working electrode used was the polished end of a polycrystalline Au wire 1 mm in diameter. The electrode was polished with emery paper (no. 10000). After a mirrorlike surface was obtained, it was rinsed ultrasonically in purified water for one minute. Then it was electrolyzed in a deoxygenated 1 M H_2SO_4 aqueous solution until the typical current−voltage (CV) curve for the Au electrode was observed. The potential was controlled by a potentiostat (HA-301, Hokuto Denko). A Ag/AgCl (3 M NaCl) electrode (RE−1B, BAS Co. Ltd.) and a coil of Pt wire 1 mm in diameter were used as the reference and counter electrodes, respectively.

3. Results

Figure 1 shows an ESR spectrum observed by UV irradiation of a TiO_2 suspension with HTMP. The ESR signals centered at $g = 2.006$ are consistent with hyperfine coupling with one ^{14}N and six ^1H. The coupling constants for a_N and a_H are 1.72 and 0.046 mT, respectively. This spectrum is identical to that of the commercially available reagent of TEMPOL radical. Since TEMPOL takes the chair conformation in the puckering of the six-membered ring, the six protons of the two equatorial methyl groups are responsible for the small coupling observed. Thus, similar to the reported formation of 4-oxo-TEMPO (Scheme 1), the photocatalytic formation of TEMPOL from HTMP, (Scheme 2A), was confirmed.

Figure 2 shows time profiles of the ESR signal for the TEMPOL radical under UV irradiation of different intensities. With increasing UV intensity, the formation rate becomes large,

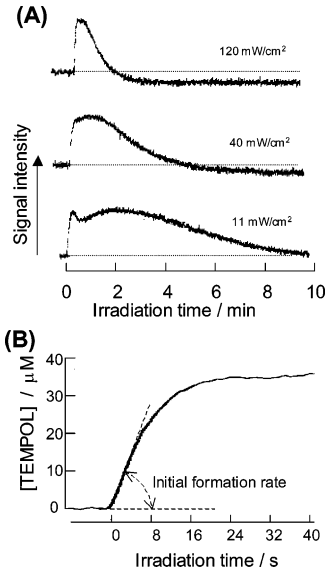

Figure 2. ESR signal intensity of the low field peak of TEMPOL radical observed on the UV irradiation on 6 g/L TiO_2(P25) aqueous suspension containing 0.5 M HTMP: (A) irradiation with three different light intensities; (B) expansion in the recording for 40 mW/cm^2. The axis of signal intensity has been converted into the scale of TEMPOL concentration. The gradient of initial increase gives the formation rate of the radical.

corresponding to the increase in the excitation of TiO_2. The increase of the decay rate with irradiation intensity indicates that the excitation of TiO_2 is involved with the decrease in the amount of TEMPOL radical. That is, the formed TEMPOL radical is subjected to the photocatalytic reaction. The decay of the TEMPOL radical in TiO_2 photocatalytic systems has been reported previously,[17] since the decay of nitroxide radicals has been reported as a detection method for ·OH radicals in photocatalytic reactions.[19] In addition to the ·OH radical, $\cdot O_2^-$ is also considered as a reactant in the decay of nitroxide radicals,[6,20] as shown in Scheme 2B.

When the light intensity was low, for example, 11 mW cm^{-2}, two peaks in the signal intensity for TEMPOL were observed in the time profile in Figure 2A. This experimental result indicates that there are two reaction processes in the formation and decay of TEMPOL. Upon irradiation at 40 mW cm^{-2}, the maximum concentration was observed after 50 s irradiation. The maximum concentration did not vary with the excitation intensity, suggesting that same photocatalytic reaction is involved with the growth and decay of TEMPOL.

When the amount of HTMP was decreased at the fixed light intensity of 40 mW cm^{-2}, the maximum amount of TEMPOL decreased, while the time to attain the maximum concentration (50 s) was not changed. The maximum amount of TEMPOL was plotted in Figure 3 as a function of the HTMP concentration for three types of photocatalytic TiO_2. The amount of TEMPOL radicals increased almost linearly with the HTMP concentration up to 0.5 M.

Detailed analysis of the time profiles for TEMPOL concentration similar to those shown in Figure 2A may provide definite information about the reaction mechanism. However, the reaction processes become complicated with the reaction intermediates produced by the irradiation. Thus, in the present study, to simplify the analysis, only the initial formation rate was measured in the subsequent experiments. To measure the initial formation rates, the scales for both the signal and irradiation time in the ESR measurement were enlarged to obtain

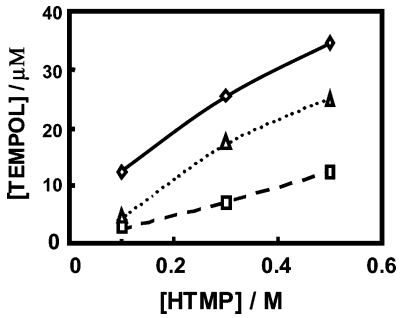

Figure 3. Effect of HTMP concentration on the maximum concentration of the TEMPOL radical observed with 40 mW/cm^2 irradiation on the suspension of three different TiO_2 photocatalysts: P25 (◊), UV-100 (△), and AMT-600 (□).

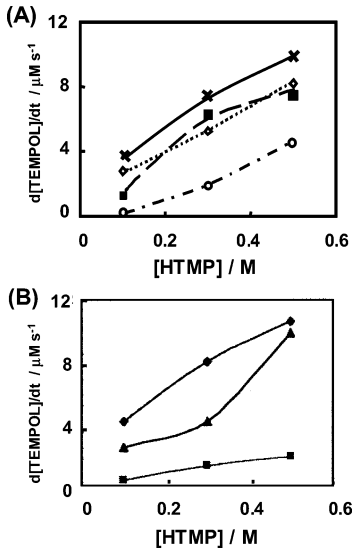

Figure 4. Formation rate of TEMPOL radical as a function of HTMP concentration. Panel A shows the effect of the amount of TiO_2 (P25) concentration on the TiO_2 concentrations: 2 (◊), 3 (■), 6 (×), and 12 (○) g/L. Panel B shows the effect of the kind of TiO_2 photocatalysts other than P25 (♦): UV-100 (▲) and AMT-600 (■). The amount of TiO_2 was 6 g/L.

the linear fits. Figure 2B shows an example of the measurement of initial rate of TEMPOL radical formation.

Figure 4A shows the initial formation rate of TEMPOL radical with various concentrations of TiO_2 powders. The formation rate increased with increasing TiO_2 concentration up to 6 g/L (L = dm^3). However, it decreased at higher concentrations, because the light absorption was limited near the front surface and the light scattering increased. From this result, we used 6 g/L as a standard concentration of TiO_2 particles in the subsequent experiments. The apparent quantum efficiency for radical formation was estimated to be about 0.1%, on the basis of the initial formation rate of 10 μMs^{-1} and the incident light intensity of 40 mW cm^{-2}. The actual quantum yield is larger than this value, since the light path length was too thin to absorb all of the incident light, and a significant amount of the incident light was scattered by TiO_2 particles at higher concentrations.

Figure 4B shows the initial formation rates of the TEMPOL radical for three different TiO_2 photocatalysts (P25, UV-100, and AMT-600) as a function of the HTMP concentration. Since the experimental uncertainty depends on the photocatalyst as stated above, nonlinear trace observed for UV-100 stems from the scattering experimental data. This plot for the initial formation rate correlates well with that for the maximum concentration of TEMPOL in Figure 3, indicating that a

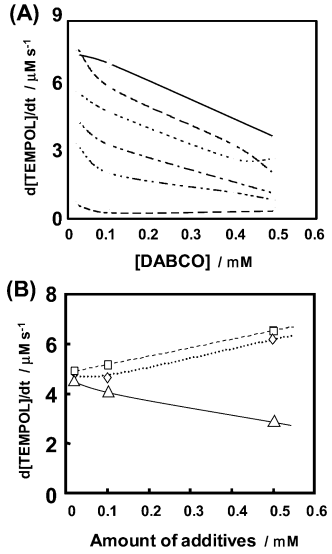

Figure 5. Effect of various additives on the photocatalytic formation rate of TEMPOL with 6 g/L TiO_2 aqueous suspension. Panel A shows DABCO for various TiO_2 photocatalysts: P25 (◇), F4 (○), ST-21 (+), AMT-600 (□), AMT-100 (×), and MTB-500B (△). (B) Additives are KSCN (□), KI (◇), and methanol (△) with P25 TiO_2 photocatalyst.

particular reaction process is common in the photocatalytic reaction processes for these TiO_2 photocatalysts.

Assuming that the key reactant in the TEMPOL formation is $^1O_2$, we added a quenching reagent, DABCO, in the reaction systems for the six different photocatalysts with similar particle sizes of larger than 20 nm. MT-500B is a TiO_2 consisting of 100% rutile, and F4 contains 10% rutile crystal with 90% anatase. The others are 100% anatase TiO_2. As shown in Figure 5A, the initial formation rate decreased by the addition of DABCO, except for MT-500B TiO_2. For MT-500B, the formation rate was too low to evaluate the decrease. Since DABCO deactivates $^1O_2$, this observation may be consistent with the assumption that the active species in the formation of TEMPOL radical is $^1O_2$.

Figure 5B shows the effect of I^-, SCN^-, and methanol on the initial formation rates of TEMPOL. When I^- and SCN^- ions were added, the formation rates increased. In our previous report, the amount of $\cdot O_2^-$ in TiO_2 suspensions decreased with the addition of I^- and SCN^-.[16] In our recent observations of $^1O_2$ phosphorescence,[18] the amount of $^1O_2$ decreased with the addition of I^- and SCN^-. Therefore, the present observation does not support the idea that $\cdot O_2^-$ or $^1O_2$ is the key reactant in the formation of TEMPOL.

With the addition of methanol, the reaction rate decreased, as shown in Figure 5B. This observation is consistent with a report for ethanol[13] in which the formation of nitroxide radicals was not observed in ethanol suspensions of TiO_2. Since $^1O_2$ does not react with alcohols,[21] if the key reactant is $^1O_2$, the decrease of $^1O_2$ may be explained by the consumption of holes by the oxidation of alcohol molecules or by the consumption of O_2 by the oxidized alcohol radicals.

Figure 6 shows the effect of H_2O_2 on the initial formation rates for the TEMPOL radical and 4-oxo-TEMPO radical from HTMP and 4-oxo-TMP, respectively, where the concentration of 4-oxo-TMP was one-fifth of that of HTMP owing to limited solubility. Similar to the dependence on the formation of $\cdot O_2^-$ and $\cdot OH$[16] by the addition of very small amounts of H_2O_2, the formation rate increased. At higher concentrations (starting at about 0.4 mM), the formation rates began to decrease. In the case of $\cdot OH$, no decrease was observed.[16] It should be noted

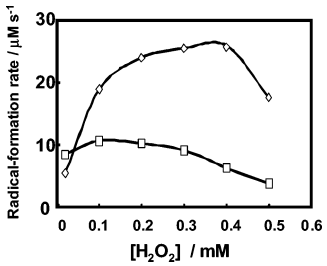

Figure 6. Effect of H_2O_2 on the formation rates of TEMPOL and 4-oxo-TEMPO radicals from 0.5 M HTMP (□) and 0.1 M 4-oxo-TMP (◇), respectively, in 6 g/L TiO_2 (P25) photocatalyst suspension.

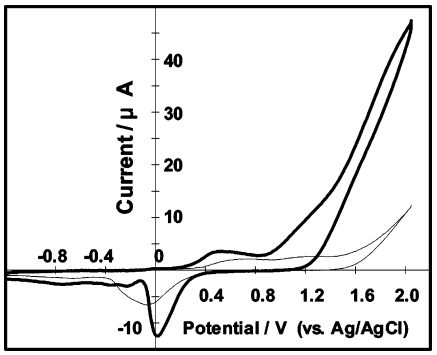

Figure 7. Cyclic voltammetry curves of aqueous solution of pH 12 with NaOH in the absence of HTMP (fine line) and in the presence of 0.05 M HTMP (bold line).

that the concentration corresponding to the maximum formation rate changed with the type of sterically hindered cyclic amine. If the key reactant of TEMPOL formation simply reacted with H_2O_2, a similar dependence on H_2O_2 concentration would be expected. Thus, the observed difference in the dependence on H_2O_2 concentration indicates that H_2O_2 is involved with a reaction with the cyclic amines, because the concentrations of amines were different.

When D_2O was used in place of H_2O, the formation rate decreased to one-third. This observation is consistent with a report by Konaka et al. in which the concentration of formed 4-oxo-TEMPO radical decreased by one-third in D_2O.[13] If the active species is $^1O_2$, the rate is expected to either increase or be unchanged, because the lifetime of $^1O_2$ in D_2O is longer by 20 times than that in H_2O.[22]

To elucidate the oxidation of HTMP on TiO_2 surface, we measured the electrochemical redox properties by means of cyclic voltammetry. Figure 7 shows that HTMP is oxidized at the potential of 0.5 V and oxidized further by two different steps between 0.9 and 2.0 V (vs Ag/AgCl). The first oxidation potential (0.7 V vs NHE) is sufficiently low that HTMP should be easily oxidized by valence band holes (−2.5 V) or even trapped holes of TiO_2.[23]

4. Discussion

To specify the key species for TEMPOL radical formation for HTMP in the TiO_2 photocatalytic system, we measured the formation rates of the radical under various conditions. The experimental results in Figures 5A indicate that the key species should be $^1O_2$ as indicated in the literature.[13−15] On the other hand, the data in Figures 6 and 7 contradict this assumption. For the moment, we let the active species to form TEMPOL from HTMP be indicated as X. Species X can be identified from the experimental observations under various conditions.

A simplified reaction scheme can be presented as follows. The unknown active species X is formed with light irradiation

TABLE 1: Reaction Rate Constants of Supposed Active Species for the Intrinsic Decay (k_0), and for the Reactions with HTMP (k_H) and Several Types of Additives (k_A)

supposed active species, X	k_0 (s^{-1})	k_H (M^{-1} s^{-1})	k_A (M^{-1} s^{-1})				
			DABCO	I^-	SCN^-	CH_3OH	H_2O_2
$^1O_2$	5×10^5 [a]	5.0×10^7 [b]	2.9×10^8 [c]	8.7×10^5 [d]		3×10^3 [e]	
$\cdot O_2^-$	$<2 \times 10^4$ [f]	1.7×10^3 [g]	~ 0 [h]	~ 0 [i]	~ 0 [i]	~ 0 [j]	0.13 [k]
$\cdot OH$	$\sim 10^5$ [l]	1.8×10^{10} [m]	1.3×10^9 [n]	1.1×10^{10} [o]	1.1×10^{10} [o]	9.7×10^8 [o]	2.7×10^7 [o]
h^+	$\sim 10^{11}$ [p]	$\sim 10^{10}$ [q]	$\sim 10^{10}$ [q]	$\sim 10^{10}$ [q]	$\sim 10^{10}$ [q]	3.3×10^9 [r]	

[a] Reference 18. [b] Reference 24. [c] Reference 25. [d] Reference 26. [e] Reference 21. [f] In aqueous TiO_2 powder suspension.[16] [g] For 2,2,6,6-tetramethyl piperidine 1-ol.[27] [h] No reaction.[27] [i] <0.014 for Cl^-.[28] [j] Reference 29. [k] Reference 30. [l] Decay by biradical recombination of 1 μM $\cdot OH$.[31] [m] For di-butylamine.[31] [n] Reference 32. [o] Reference 31. [p] From the lifetime of a few ps.[33] [q] Assuming the diffusion limit bimolecular reaction. [r] In the unit of s^{-1} from the lifetime of h^+ in CH_3OH.[34]

at the rate g.

$$TiO_2 + h\nu \xrightarrow{g} X \quad (1)$$

Since the excitation light intensity was constant during the reaction, the rate g was constant. It is assumed that X plays a role in forming TEMPOL from HTMP with the initial rate constant k_H.

$$X + HTMP \xrightarrow{k_H} TEMPOL \quad (2)$$

In the absence of HTMP, the active species X can be deactivated with the rate constant k_0:

$$X \xrightarrow{k_0} \text{deactivation} \quad (3)$$

In the present study, additives are used to help to identify X. A particular additive, Add, reacts with the active species X at a rate with rate constant k_A.

$$X + Add \xrightarrow{k_A} \text{deactivation} \quad (4)$$

From the above assumptions, the rate equation for the formation of X is given by

$$d[X]/dt = g - k_0[X] - k_H[X][HTMP] - k_A[X][Add] \quad (5)$$

The above equations well describe the present experimental data, since the discussion in the present work is confined to the initial growth rates of TEMPOL radical with UV irradiation. The formation of species X begins only with irradiation; that is, $[X] = 0$ at $t = 0$. By adopting this boundary condition, eq 5 can be integrated to give

$$[X] = g(1 - \exp(-(k_0 + k_H[HTMP] + k_A[Add])t))/(k_0 + k_H[HTMP] + k_A[Add]) \quad (6)$$

According to the simplified reaction 2, the formation rate of TEMPOL can be given by

$$d[TEMPOL]/dt = k'_H[X][HTMP] \quad (7)$$

Here, k'_H represents the effective rate constant for the formation of TEMPOL. When the reaction of X with HTMP is the rate-determining step, k'_H becomes nearly equal to k_H.

Then, from eqs 6 and 7, the formation rate of TEMPOL is given by

$$d[TEMPOL]/dt = gk'_H[HTMP](1 - \exp(-(k_0 + k_H + [HTMP] + k_A[Add])t))/(k_0 + k_H[HTMP] + k_A[Add]) \quad (8)$$

Since the initial growth of TEMPOL observed was a linear line for all measurements, eq 8 is independent of time. That is, $1 \gg \exp(-(k_H[HTMP] + k_A[Add] + k_0)t)$. Therefore, under the experimental conditions, eq 8 can be simplified to give

$$d[TEMPOL]/dt = gk'_H[HTMP]/(k_0 + k_H[HTMP] + k_A[Add]) \quad (9)$$

This equation might express the dependence of the initial formation rate of TEMPOL on the concentrations of HTMP and the additives, such as DABCO, I^-, SCN^-, methanol, and H_2O_2. However, care should be taken that the rate g for X generation and the effective rate constant k'_H for TEMPOL formation could possibly be changed in the presence of these additives.

As mentioned in the Introduction, the candidates of X are $^1O_2$, $\cdot O_2^-$, $\cdot OH$, and h^+. In Table 1 are listed the reported rate constants of k_0, k_H, and k_A for these species. As for the rate constants of reaction with h^+, though there are few reports thus far, the rate constant is probably almost at the diffusion limit (ca. 10^{10} M^{-1} s^{-1}).

As shown in Figure 4, the rate of TEMPOL formation increased almost linearly with HTMP concentration up to 0.5 M. Since $[Add] = 0$ in this case, the observation in Figure 4 gives the relationship that $k_0 \gg k_H[HTMP]$ from eq 9. That is, the formation of TEMPOL (eq 2) is not the dominant process for the decay of X, but the decay by eq 3 with the rate constant k_0 is. From Table 1, if X is $\cdot O_2^-$ or h^+, the relation that $k_0 \gg k_H[HTMP]$ could hold, but it is not consistent if $^1O_2$ or $\cdot OH$ are assigned to X.

Figure 5A shows that the formation rate of TEMPOL decreased to about half by the addition of 0.5 mM DABCO. This indicates that the intrinsic decay of X (eq 3) and the decay of X by the reaction with DABCO become parallel. That is, $k_A[DABCO]$ become equal to k_0 at 0.5 mM DABCO. From this relationship, the reaction rate constant k_A is estimated to be 1×10^9 M^{-1} s^{-1}. Since this value is 3.4 times larger than the reported quenching rate in Table 1, the active species X is not likely to be $^1O_2$.

The addition of SCN^- and I^- increased the formation rate of TEMPOL radicals, as shown in Figure 5B. As will be reported elsewhere, the phosphorescence intensity of $^1O_2$ decreased by the addition of these ions, indicating that the formation rate g for $^1O_2$ is decreased with SCN^- and I^-. Thus, the increase in the formation rate with these ions contradicts the assumption that $^1O_2$ is the active species X. Since the amount of $\cdot O_2^-$ produced decreased with these ions,[16] $\cdot O_2^-$ is not the active species for TEMPOL formation. The photoinduced holes react with SCN^- and I^-, which then proceed to form the dihalide radical ions, $\cdot (SCN)_2^-$ and $\cdot I_2^-$, respectively. These dihalide radical ions have oxidation potentials of 1.64 and 1.35,

respectively.[35] These radical ions could oxidize HTMP to produce TEMPOL radicals.

$$\mathrm{HTMP} + \cdot(\mathrm{SCN})_2^- \rightarrow \mathrm{HTMP}^+ + 2\mathrm{SCN}^- \qquad (10)$$

Here, $HTMP^+$ represents a transient oxidized state of HTMP and may be identical to the product of the reaction of HTMP and h^+. Thus the increase in the TEMPOL formation rate with these ions could be explained.

By the addition of methanol, the formation rate of TEMPOL decreased (Figure 5B), contrary to the cases of SCN^- and I^-. If the oxidation of HTMP competes with that of methanol, the formation rate of TEMPOL would decrease on the addition of methanol. The formation rate g for other supposed reactive species may also decrease. Thus, from the decrease of the formation rate with the addition of methanol, we could obtain no clear information with which to identify X.

As shown in Figure 6, when increasing amounts of H_2O_2 were added, the growth rate of TEMPOL radical increased slightly at first but then decreased at concentrations above 0.2 mM. Although this increase is very similar to that observed for $\cdot O_2^-$,[15] X is not assigned to $\cdot O_2^-$, because the concentration dependence is different from that of 4-oxo-TMP. In the case of 4-oxo-TMP by the addition of H_2O_2, the formation rate of nitroxide radical increased by 5 times at 0.4 mM H_2O_2. If H_2O_2 influences only the formation rate of X, the profiles in Figure 6 should be similar to each other. Therefore, the effect on the formation rate with H_2O_2 is due to the reaction of H_2O_2 with $HTMP^+$ to produce TEMPOL.

In the above discussion on the experimental observations with the additives, X is most likely trapped holes. If we assume a diffusion-limited reaction of HTMP with the active species X, $k_H = 10^{10}\ M^{-1}\ s^{-1}$, the pseudo-first-order reaction rate (k_1-[HTMP]) is calculated to be $5 \times 10^9\ s^{-1}$. This value is smaller than k_0, which is the order of $10^{11}\ s^{-1}$, because hole transfer at the TiO_2 surface takes place in a few ps, as reported from femtosecond laser experiments.[33] Therefore, X is likely to be the trapped hole.

Since HTMP is oxidized at the electrode potentials at 0.7 V (vs NHE), as shown in Figure 7, it could be directly oxidized by TiO_2 photocatalysts. That is, this observation supports the above conclusion that the active species X is most likely the photoinduced valence band hole or trapped hole. It was reported that the radical cation of TMP formed in Freon-113 glass matrix at 77 K deprotonated during annealing at 104 K to form the TEMPO radical by reaction with molecular oxygen.[12] A similar reaction could take place in the TiO_2 photocatalytic reaction with HTMP, as shown in Scheme 3. That is, the photogenerated valence band holes or trapped holes, h^+, oxidize HTMP to form piperidyl radicals, followed by reaction with O_2 to become peroxide radicals, and finally TEMPOL radical is formed by disproportionation.

5. Conclusions

The key species X in the formation process of TEMPOL from HTMP in TiO_2 photocatalytic system was investigated on the basis of the changes of the formation rate with various additives. The candidates of the key species were $^1O_2$, $\cdot O_2^-$, $\cdot$OH, valence band holes (or surface trapped holes, h^+).

The key species is not $^1O_2$, because of the following two observations. In Figure 4, the increase of the rate with HTMP, that is $k_0 \gg k_H$[HTMP], could not be supported; besides, the generation of $^1O_2$, g, is not likely to increase with HTMP. In Figure 5B, the formation rate of TEMPOL increased with the addition of SCN^- and I^-, while the amount of $^1O_2$ measured with phosphorescence intensity[18] was decreased.

SCHEME 3

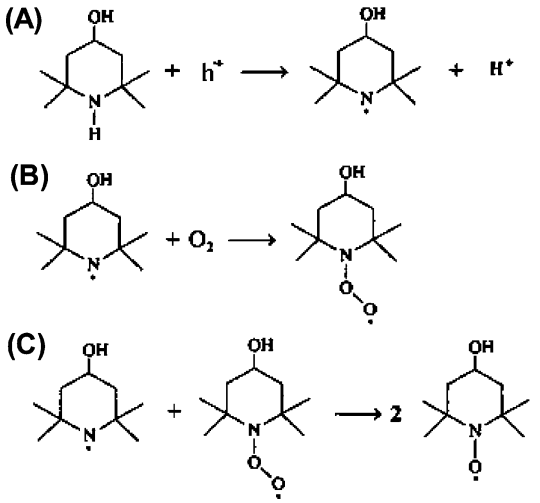

The key species is not $\cdot O_2^-$, because of the observation that the TEMPOL formation rate decreased upon addition of DABCO and methanol (Figure 5), even though these molecules do not react with $\cdot O_2^-$. Since these molecules could be oxidized in the photocatalytic reaction, the addition of such small amounts of reactant may cause the increase of the formation of $\cdot O_2^-$ in the photocatalytic reduction. Therefore, the g for $\cdot O_2^-$ could not decrease.

The key species is not $\cdot$OH. Since the rate constant of k_H for $\cdot$OH is diffusion-limited, the relation, $k_0 \gg k_H$[HTMP], which is observed in Figure 4B, could not be explained. It is difficult to explain Figure 5B, in which the increase was observed by the addition of oxidizable SCN^- and I^-, because the increase in the g for $\cdot$OH with the addition of the reactants could not be explained. Furthermore, as reported in the previous paper, the formation of $\cdot$OH in TiO_2 photocatalytic systems is still problematic.[17,23]

If the key species X is assumed to be h^+, all of the experimental observations can be explained. The electrochemical measurements support the direct oxidation of HTMP. Also, the reaction process from oxidized HTMP to TEMPOL with molecular oxygen, O_2, is clearly elucidated from a low-temperature ESR study.[12] The reaction with O_2 could occur at the surface of TiO_2. Then, the significant increase with the addition of H_2O_2 could be explained by the increase of surface adsorbed O_2. The difference between TEMPOL and 4-oxo-TEMPO in Figure 6 corresponds to the stability of the oxidized amine radical in Scheme 3B.

In short, the significant observations in the present study were the increase of the formation rate with the HTMP concentration, even at 0.5 M (Figure 4), and the increase with the addition of SCN^- and I^- (Figure 5B). From these observations, it is concluded that HTMP is directly oxidized with holes in the excited TiO_2 to produce the TEMPOL radical, and the reaction with the other reactive species, such as $^1O_2$, $\cdot O_2^-$, and $\cdot$OH is not the dominant process. Since ESR spectroscopy is more sensitive than other spectroscopic methods for the detection of TEMPOL, this reaction provides a powerful method to evaluate the oxidation activity of photocatalysts.

Acknowledgment. This work was supported in part by a Grant-in-Aid on Priority Areas (417) from the Ministry of Education, Culture, Science and Technology (MEXT) and also

by Core Research for Evolution Science and Technology (CREST), under the auspices of the Japan Science and Technology Agency (JST). The authors thank Dr. D. A. Tryk for his help to edit the manuscript.

References and Notes

(1) Fujishima, A.; Rao, T. N.; Tryk, D. A. *J. Photochem. Photobiol., C* **2000**, *1*, 1−21.
(2) *Handbook of Heterogeneous Catalysis;* Ertl, G., Kneinger, H., Weitkamp, J., Eds.; Wiley-VCH: Weinheim, Germany, 1997.
(3) *Photocatalysis;* Kaneko, M., Ohkura, I., Eds.; Kodansha-Springer, Tokyo, 2002.
(4) Horikoshi, S.; Watanabe, N.; Mukae, M.; Hidaka, H.; Serpone, N. *New J. Chem*. **2001**, *25*, 999−1005.
(5) Liauw, C. M.; Quadir, A.; Allen, N. S.; Edge, M. *J. Vinyl Addit. Technol*. **2004**, *10*, 159−167.
(6) Kocherginsky, N. *Nitroxide Spin Labels: Reactions in Biology and Chemistry*; CRC Press: Boca Raton, FL, 1995.
(7) Nakahara, K.; Iwasa, S.; Satoh, M.; Morioka, Y.; Iriyama, J.; Suguro, M.; Hasegawa, E. *Chem. Phys. Lett.* **2002**, *359*, 351−354.
(8) Rosenthal, I.; Murali Krishna, C.; Yang, G. C.; Kondo, T.; Riesz, P. *FEBS Lett*. **1987**, *222*, 75−78.
(9) Lion, Y.; Delmelle, M.; Van de Vorst, A. *Nature*, **1976**, *263*, 442−443.
(10) Mothilal, K. K.; Johnson Inbaraj, J.; Gandhidasan, R.; Murugesan, R. *J. Photochem. Photobiol., A* **2004**, *162*, 9−16.
(11) Poupko, R.; Rosenthal, I. *J. Phys. Chem.* **1973**, *77*, 1722−1724.
(12) Goettinger, H. A.; Zubarev, V. E.; Brede, O. *J. Chem. Soc., Perkin Trans.* 2 **1997**, 2167−2172.
(13) Konaka, R.; Kasahara, E.; Dunlap, W. C.; Yamamoto, Y.; Chien, K. C.; Inoue, M. *Redox Rep.* **2001**, *6*, 319−325.
(14) Barclay, L. R. C.; Basque, M.-C.; Vinqvist, M. R. *Can. J. Chem*. **2003**, *81*, 457−467.
(15) Konovalova, T. A.; Lawrence, J.; Kispert, L. D. *J. Photochem. Photobiol., A* **2004**, *162*, 1−8.
(16) Hirakawa, T.; Nosaka, Y. *Langmuir*, **2002**, *18*, 3247−3254.
(17) Nosaka, Y.; Komori, S.; Yawata, K.; Hirakawa, T.; Nosaka, A. Y. *Phys. Chem. Chem. Phys*. **2003,** *5*, 4731−4735.
(18) Nosaka, Y.; Daimon, T.; Nosaka, A. Y.; Murakami, Y. *Phys. Chem. Chem. Phys.* **2004**, *6*, 2917−2918.
(19) Schwarz, P. F.; Turro, N. J.; Bossmann, S. H.; Braun, A. M.; Abdel Wahab, A. A.; Duerr, H. *J. Phys. Chem. B* **1997**, *101*, 7127−7134.
(20) Yamakoshi, Y.; Umezawa, N.; Ryu, A.; Arakane, K.; Miyata, N.; Goda, Y.; Masumizu, T.; Nagano, T. *J. Am. Chem. Soc.* **2003**, *125*, 12803−12809.
(21) Schmidt, R.; Afshari, E. *Ber. Bunsen-Ges. Phys. Chem*. **1992**, *96*, 788−794.
(22) Schweitze, C.; Schmidt, R. *Chem. Rev*. **2003**, *103*, 1685−1757.
(23) Nakamura, R.; Nakato, Y. *J. Am. Chem. Soc*. **2004**, *126*, 1290−1298.
(24) Kamath, S. S.; Srivastava, T. S. *J. Photochem. Photobiol*., A **1990**, *52*, 83−89.
(25) Iu, K.-K.; Thomas, J. K. *J. Photochem. Photobiol*., A **1993**, *71*, 55−60.
(26) Braathen, G.; Chou, P.-T.; Frei, H. *J. Phys. Chem*. **1988**, *92*, 6610−6615.
(27) Bielski, B. H. J.; Cabelli, D. E.; Arudi, R. L.; Ross, A. B. *J. Phys. Chem. Ref. Data* **1985**, *14*, 1041−1100.
(28) Long, C. A.; Bielski, B. H. J. *J. Phys. Chem*. **1980**, *84*, 555−557.
(29) McDowell, M. S.; Bakac, A.; Espenson, J. H. *Inorg. Chem*. **1983**, *22*, 847−848.
(30) Weinstein, J.; Bielski, B. H. J. *J. Am. Chem. Soc*. **1979**, *101*, 58−62.
(31) Buxton, G. V.; Greenstock, C. L.; Helman, W. P.; Ross, A. B. *J. Phys. Chem. Ref. Data* **1988**, *17*, 513−886.
(32) Anderson, R. F.; Patel, K. B. *Photochem. Photobiol*. **1978**, *28*, 881−885.
(33) Yang, X.; Tamai, N. *Phys. Chem. Chem. Phys.* **2001**, *3*, 3393−3398.
(34) Tamaki, Y.; Furube, A.; Murai, M.; Hara, K.; Katoh, R.; Tachiya, M. *J. Am. Chem. Soc.* **2006**, *127*, 417−418.
(35) Wardman, P. *J. Phys. Chem. Ref. Data* **1989**, *18*, 1637−1755.